Interpretation of the CABRI LT1 Test with SAS4A-code Analysis

March, 2001

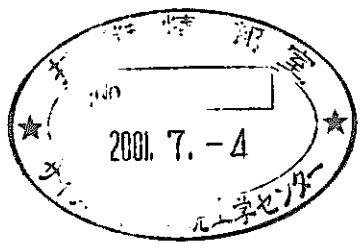

O-arai Engineering Center
Japan Nuclear Cycle Development Institute

〒319-1184　茨城県那珂郡東海村大字村松4-49
核燃料サイクル開発機構
技術展開部　技術協力課
Inquiries about copyright and reproduction should be addressed to :
Technical Cooperation Section,
Technology Management Division,
Japan Nuclear Cycle Development Institute
4-49 Muramatsu, Tokai-mura, Naka-gun, Ibaraki, 319-1184
Japan

JNC TN9400 2001-048
March, 2001

Interpretation of the CABRI LT1 test with SAS4A-code analysis

Ikken SATO[*1] and Yu-uichi ONODA[*1]

Abstract

In the CABRI-FAST LT1 test, simulating a ULOF (Unprotected Loss of Flow) accident of LMFBR, pin failure took place rather early during the transient. No fuel melting is expected at this failure because the energy injection was too low and a rapid gas-release-like response leading to coolant-channel voiding was observed. This channel voiding was followed by a gradual fuel breakup and axial relocation.

With an aid of SAS4A analysis, interpretation of this test was performed. Although the original SAS4A model was not well fitted to this type of early pin failure, the global behavior after the pin failure was reasonably simulated with temporary modifications. Through this study, gas release behavior from the failed fuel pin and its effect on further transient were well understood. It was also demonstrated that the SAS4A code has a potential to simulate the post-failure behavior initiated by a very early pin failure provided that necessary model modification is given.

---

*1: Advanced Technology Division,
O-arai Engineering Center, JNC.

JNC TN9400 2001-048
２００１年３月

Interpretation of the CABRI LT1 test with SAS4A-code analysis

佐藤一憲[*1]、小野田雄一[*1]

要旨

高速増殖炉の ULOF (Unprotected Loss of Flow) 事故を模擬した CABRI-FAST LT1 試験では、過渡中の早期の段階でピン破損を生じた。この時点での燃料へのエネルギー投入は極めて小さく、燃料は未溶融と考えられる。ピン破損後は急速なガス放出と見られる冷却材応答が観測され、流路はボイド化した。このボイド化の後、燃料は連続的に崩壊し軸方向に移動した。

本研究では SAS4A コードを用いた解析を実施し、その結果を参考にして本試験の解釈を行った。オリジナル SAS4A コードのモデルは、本試験のような燃料ピン早期破損時の破損後挙動評価には十分に対応したものではないが、本試験の状況を反映した特殊な取扱いを導入することにより、破損後の挙動を適正に模擬することができた。この研究を通じて、早期破損ピンからのガス放出挙動及びその後の挙動へのガス放出の影響が明らかになった。また、必要なモデル変更を前提として、SAS4A コードによる燃料ピン早期破損からの挙動模擬のポテンシャルを示した。

---

*1: 大洗工学センター、要素技術開発部

CONTENTS

LIST OF TABLES

LIST OF FIGURES

1. Introduction

The LT1 test was performed on December 14th 1995 as the last transient test within the framework of the CABRI-FAST program. This test was a TUCOP(Transient Under-Cooling Over-Power) aiming at investigation of fuel failure and subsequent fuel relocation within the coolant channel as well as pre-failure in-pin fuel motion with a high burn-up annular fuel.

The QUASAR pin which had been pre-irradiated up to 12 at.% of peak burn-up was used in this test. From the CABRI steady state of 465W/cm, a coolant flow reduction with a halving time of about 7 seconds was applied. TOP(Transient Over-Power) was triggered at 16.76 sec after the initiation of LOF(Loss of Flow) when coolant average temperature at the fissile top reached pre-defined value to keep the subcooled condition.

During the TOP, a rather early cladding failure took place before fuel melting and coolant boiling. This cladding failure was followed by a rapid gas release leading to coolant-channel voiding. Under the gas-induced voiding condition, continued power transient resulted in continuous fuel disruption and axial relocation similar to those in existing CABRI TUCOP tests with extended coolant boiling conditions.

In this study with the SAS4A code, it was intended to simulate the sequence of these events applying the plenum-gas-blowout model for the gas-release behavior. This type of transient sequence was the first case for our SAS4A utilization, so that some modifications to the model were necessary.

2. Overview on the test results

The Quasar fuel used in this test had a 33cm-long lower blanket made of annular pellets with a central hole similar to that of the fissile region. Upper blanket was absent in this fuel and a short annular insulator pellet was placed above the fissile. Therefore, the central hole of the fissile region was initially connected to the upper and lower gas plena through the central holes. Especially in the upper part, fissile top was just in front of the upper plenum. It is considered, therefore, that such fuel design will enhance the potential of pre-failure in-pin fuel motion provided that pin failure takes place after fuel melting.

TOP was triggered automatically during LOF with the average TFC coolant temperature of 888 degree C. 385ms after the TOP, pin failure was detected by microphones and evaluated failure level was about 48cmBFC(cm above Bottom of Fissile Column) (X/L=0.56). At this time, energy injection at the PPN(Peak Power Node) was only 0.323kJ/g and fuel melting could hardly be reached. Thermocouples at 52cmBFC measured coolant temperature between

710 and 770 degree C at the failure time, so that coolant boiling before cladding rupture can be excluded.

The cladding rupture was immediately followed by sodium ejection measured by flowmeters. This sodium-ejection phase led to coolant-channel voiding within about 100~200ms as can be seen from Fig.1. During an early part of this void-development phase, thermocouples showed mostly subcooled condition except for the axial level just near the failure location indicating that the coolant channel was filled with non-condensable gas.

During a later part of this void-development phase, a gradual fuel-signal increase corresponding probably to a global fuel swelling was observed with the hodoscope in 170~390mmBFC starting at about 465ms, i.e., about 80 ms after cladding rupture.

The zone of probable fuel swelling expanded axially and mild axial relocation took place at the last stage of transient. Because of the limited energy injection, fuel disruption and axial relocation was finally limited within the fissile region.

3. Analytical condition and assumptions

In this study, the SAS4A code version "REF96 Release 1", which is commonly applied for the CABRI-FAST synthesis work in JNC, is adopted. Although considerable modifications have been given to the latest code versions concerning the fuel pin mechanics and in-pin fuel motion, the model of fuel disruption and relocation within the coolant channel is basically unchanged from this former code version. Therefore, experience in this study using the former code version seems quite applicable to the latest versions.

In the LT1 experiment, rather early cladding failure was observed. A separate study on this test using the PAPAS-2S code focusing on pin mechanics up to failure showed that the observed early failure was not well explained with the PCMI(Pellet Cladding Mechanical Interaction) characteristic expected from the CABRI-FAST PF2 and LT2 tests where pure TOP was applied using also the QUASAR fuel. Therefore, some special effect may have been operational in this TUCOP test such as pin bending specific to the CABRI single pin condition.

In the SAS4A model, failure prediction is linked to post-failure molten fuel ejection and its interaction with coolant and/or coolant-channel structures. Under this background, cladding failure with single-phase-coolant condition is allowed only after some fuel melting.

Therefore, in order to simulate the early cladding failure and gas release, a special treatment is necessary. The plenum-gas-blowout model, which is

usually applied after coolant voiding, is used for this gas release phase in this study. In order to simulate the LT1 test condition, some modifications were necessary to the SAS4A model, which are described in Appendix. Input parameters specifically selected in this study are presented in Table 1.

Cladding failure time and location, i.e., 385ms after TOP onset and ~50cmBFC, are given as the boundary condition for the plenum-gas-blowout model. Failure-rip area and orifice coefficient, which are used for pressure loss and gas-flow calculation at the failure rip, can be specified by input data. The input data for the rip area and orifice coefficient are selected so as to get reasonable simulation of the initial channel-voiding behavior.

Concerning the coolant-dynamics calculation, disappearance of liquid slug from the test channel results in an error. This is linked to the insufficient representation of the entire CABRI sodium loop including the by pass flow as well as inlet and outlet sodium channels. Therefore, in order to avoid this trouble, disappearance of the liquid slug is prevented in this study, adopting a high value for the inlet orifice coefficient and limited amount of total gas available for blowout.

For the usual coolant-boiling behavior, remaining liquid films on the cladding and structure wall are available and input-specified values are applicable. However, because of the fact that gas blowout has much more dynamic void development than usual boiling, remaining liquid films can be much thinner. In order to reflect this characteristic, film thickness of 1.0E-5 m is used both for cladding and structure. In accordance with this input selection, film-thickness values for dryout judgement are set to 0.67E-5 m to avoid unexpected dryout. With this condition, cladding facing the gas bubble becomes almost adiabatic against the gas bubble. Because of the low thermal inertia of the thin sodium film on the cladding, dryout prediction in the present study only shows that cladding temperature reaches certain level.

After the gas blowout, fuel disruption under a rapid cladding heat-up and fuel melting is expected. Criteria for fuel disruption in this phase adopted in this study are 20%AMF (fuel areal melt fraction) and cladding midwall temperature of 1250 degree C. It should be noted that this cladding-temperature level is usually reached just after cladding dryout in the conventional situations. These criteria for fuel failure are same as those in the LT4 study using SAS4A[1].

4. Calculated results

4-1 Gas blowout behavior

Calculated coolant temperature during LOF at TFC is compared with the

thermocouple data in Fig.2. Coolant heat-up behavior during LOF seems to be well simulated in the present SAS4A case. Calculated cladding temperature distribution at 385ms when gas release started in the experiment is presented in Fig.3. Cladding temperature at the failure location is about 800 degree C and fuel temperature is far below melting as shown in Fig.4.

With the present set of rip area and orifice coefficient, the plenum gas blowout model can reasonably simulate the observed coolant-channel voiding behavior as shown in Figs. 5 and 6.

Figures 7 to 9 provide comparison of coolant-channel temperature response during the gas release phase. It can be confirmed from these figures that the SAS4A is well simulating the coolant-heatup behavior during TOP up to the gas ejection. However, there appears certain difference after gas release between measured and calculated temperature.

At TFC, calculated coolant-channel temperature decreases to 800 degree C just after the gas ejection for a very short time. This is corresponding to the upward motion of the coolant liquid slug, which has an axial temperature gradient. TC data shows also a slight temperature reduction at this moment. However, thermal inertia of TC and surrounding structure will have smoothed this temperature change in the experiment. After the liquid-slug passing, coolant channel becomes filled with released gas. As described in Appendix A, heat transfer between the ejected gas and channel structure cannot be calculated in SAS4A for the early phase due to the model limitation. With this background, channel temperature increases with a sudden step in the analysis. On the other hand, temperature increases slowly in the experiment toward the sodium-saturation level showing that the ejected gas is cooled down within the heat transfer to the surrounding structure.

Although the present simulation for the gas release does not cover the possible heating of coolant-channel structure including the pin, its effect on accident scenario seems negligible because clad heating after voiding will be dominated by heat flow from the internal fuel pellets and/or molten fuel in the coolant channel.

At 67cmBFC, temperature response similar to that of TFC can be seen both in the experiment and analysis. In the experiment, temperature increase at this level is larger than that of TFC reflecting the fact that ejected gas keeps higher temperature at the upstream location. This understanding is consolidated with the TC response at 52cmBFC, which is very near to the failure site, showing rapid temperature increase comparable to the analysis at the very beginning.

4-2 Fuel disruption and axial relocation

Development of cladding-dryout and fuel-disruption regions is presented in Fig.5. Judging from the thermocouple data, region of calculated fuel disruption seems reasonable. With the suppression for heat transfer between the gas bubble and cladding, cladding is heated adiabatically leading to the specified temperature of 1250 degree C at about 160 ms after the blowout onset. As can be seen from this figure, cladding dryout is predicted just before fuel disruption at each axial level in accordance with the cladding heat up.

Axial fuel distribution at several time intervals during TOP is presented in Fig. 10. Both hodoscope data and SAS4A result correspond to average of the mass distribution for the indicated time periods. Initiation of axial fuel relocation, gradual axial relocation under continued heating and final distribution limited to the fissile region can be well simulated. From the post-transient radiography, significant fuel swelling leading to coolant-channel flow-area reduction can be observed at the axial ends of fuel accumulations. Such fuel swelling parts are serving as blockages for higher energy mobile fuel behind them. However, axial fuel relocation is taking place within the high-enthalpy region indicating that more energy injection will lead to further axial fuel relocation. The SAS4A model can well simulate the disrupted fuel mobility dependent on the fuel enthalpy.

In the following the 'relative fuel worth', which is useful for reactor case consideration is used. This parameter is defined with integration of local fuel mass multiplied by relative local power in CABRI along the fissile height. The initial relative worth is unity and fuel mass reduction from the fissile region leads to reduced relative worth proportionally. Fuel relocation within the fissile region from high power region to low power region also leads to relative worth reduction.

Figure 11 shows relative fuel worth change during LOF and TOP. Relative fuel worth decreases already during LOF leading to ~9% of reduction. Because of the fact that no meaningful fuel loss from the fissile region nor meaningful fuel relocation within the fissile is expected during this phase, this worth reduction seems to be caused by some unknown effect, which reduces the hodoscope signal without fuel mass distribution change. Pin bending is regarded as a possible candidate for such effect.

Because of the fact that this signal decrease does not seem corresponding to real worth reduction discussed here, correction seems necessary for comparison with analytical results where the relative worth stays

unity up to fuel disruption during TOP. Therefore, special correction is given to the hodoscope signal, i.e., 9% increase for comparison with the SAS4A result.

Calculated relative fuel worth with SAS4A is compared with the corrected hodoscope data in Fig.12. Again, SAS4A can well simulate the slight worth change dominated by the limited energy injection.

5. Conclusion

Application of the plenum-gas blowout model to the early-failure-induced gas release into the unvoided coolant channel has been successfully performed. With this simulation of the gas-release phase, coolant channel voiding and subsequent cladding and fuel heat-up can be well represented. Calculated fuel disruption and axial relocation are also in reasonable agreement with the experimental observation demonstrating that the present SAS4A treatment for disrupted fuel mobility dependent on fuel enthalpy is quite applicable to the high burnup annular fuel.

This successful simulation of the fuel disruption and axial relocation starting from an early pin-failure before fuel melting in the LT1 test analysis provides a good basis for future evaluation of early-pin-failure scenario in the rector case. However, failure prediction for the PCMI failure has quite large uncertainty so that this aspect should be carefully reflected in the reactor application.

Acknowledgement

The authors express their great appreciation for Mr. Yoshiki SATO of Nuclear Engineering System Inc., who helped the analytical works and preparation of the figures.

References

[1] Y. ONODA and I. SATO, "Interpretation of the LT4 test with SAS4A-code analysis," JNC TN9400 2001-047

Table 1 SAS4A input parameters specifically selected in the present study

Objectives	Variable name	Input location	Specified value	Usual value	explanation
Control plenum gas blowout behavior	IGASRL	(51, 278)	2	-	Select the option to specify the gas blowout time
	INDFAL	(51, 283)	15	-	Node number of gas blowout location
	AGSRLS	(64, 181)	3.0E-6	-	Rip area (m2)
	GASKOR	(64, 182)	3.0	-	Orifice coefficient for gas release from the plenum
	TMFAIL(1-30)	(64, 186 – 188)	1817.14	-	Gas blowout time (sec in SAS4A time)
Avoid liquid coolant slug disappearance	XKORV(1, 2)	(64, 56)	6.4	1.6	Orifice coefficient for flowing sodium at the inlet
Suppress condensation and evaporation in LEVITATE	CFNACN	(13, 1146)	0.0	6.3E4	Sodium condensation heat transfer coefficient
	CFNAEV	(13, 1147)	1.0E-6	6.0E5	Sodium evaporation heat transfer coefficient
Control initial liquid film	WFS00	(64,77)	1.0E-5	1.19E-4	Initial film thickness on the structure (m)
	WF0	(64, 84)	1.0E-5	1.19E-4	Initial film thickness on the cladding (m)
Prevent unrealistic dryout judgement	WFMNSW	(64,76)	0.67E-5	6.0E-5	Dryout film thickness on the structure (m)
	WFMNWT	(64, 75)	0.67E-5	6.0E-5	Dryout film thickness on the cladding (m)

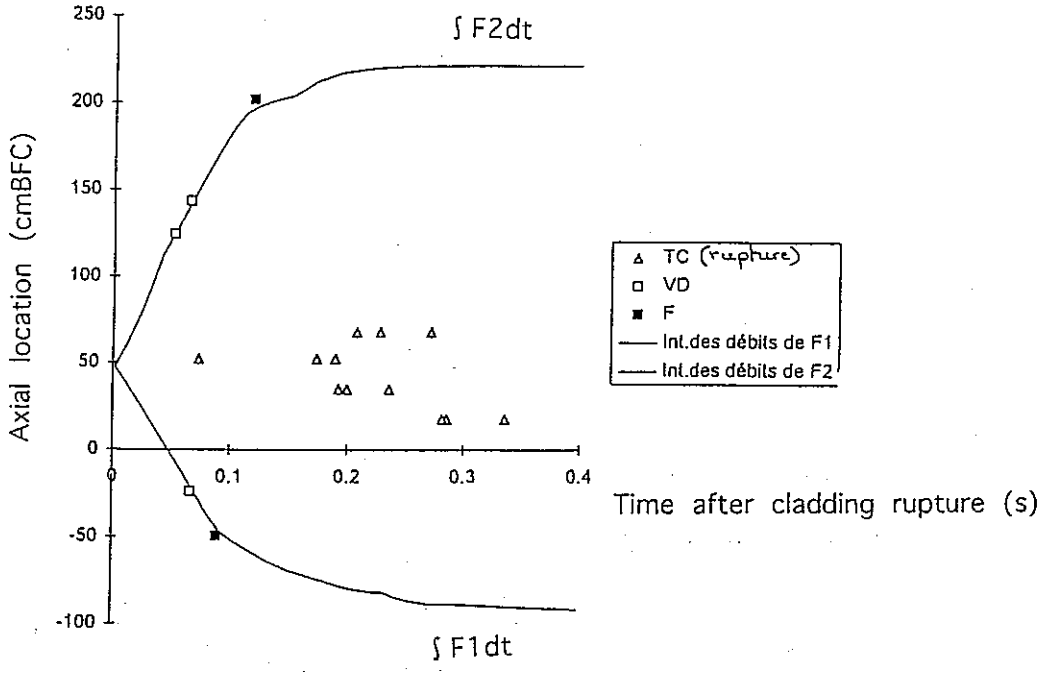

Fig.1 Coolant-channel voiding observed in the experiment during TOP

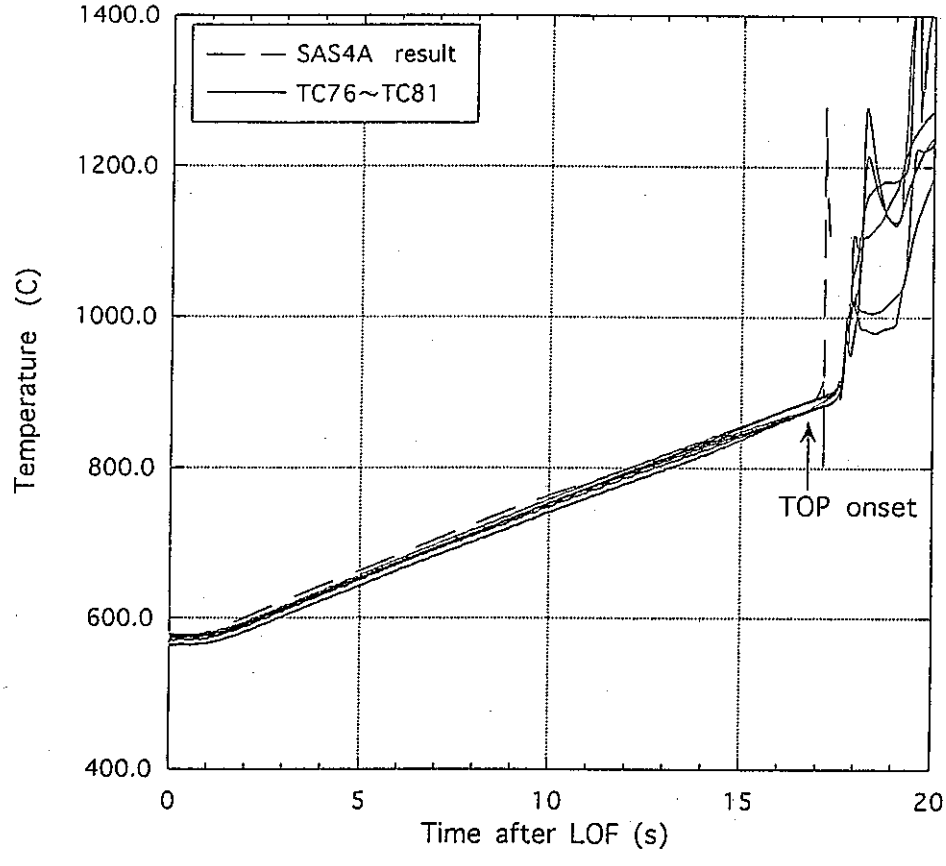

Fig.2 Coolant temperature at TFC during LOF

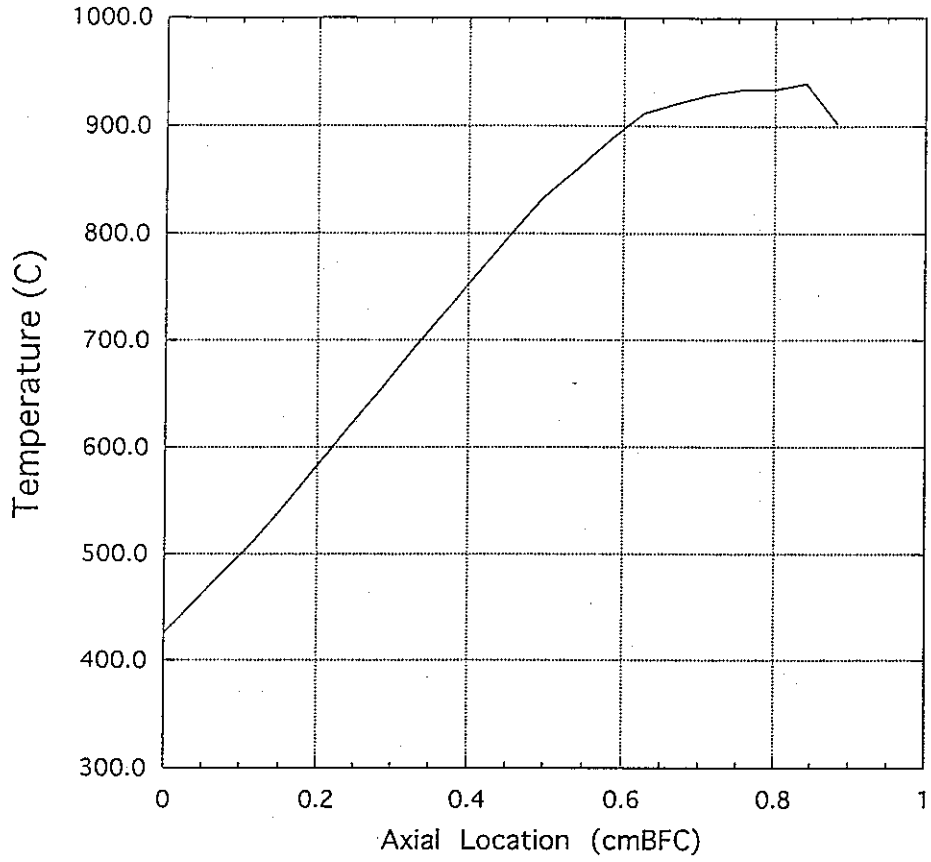

Fig.3 Calculated clad midwall temperature at 385 ms after TOP triggering

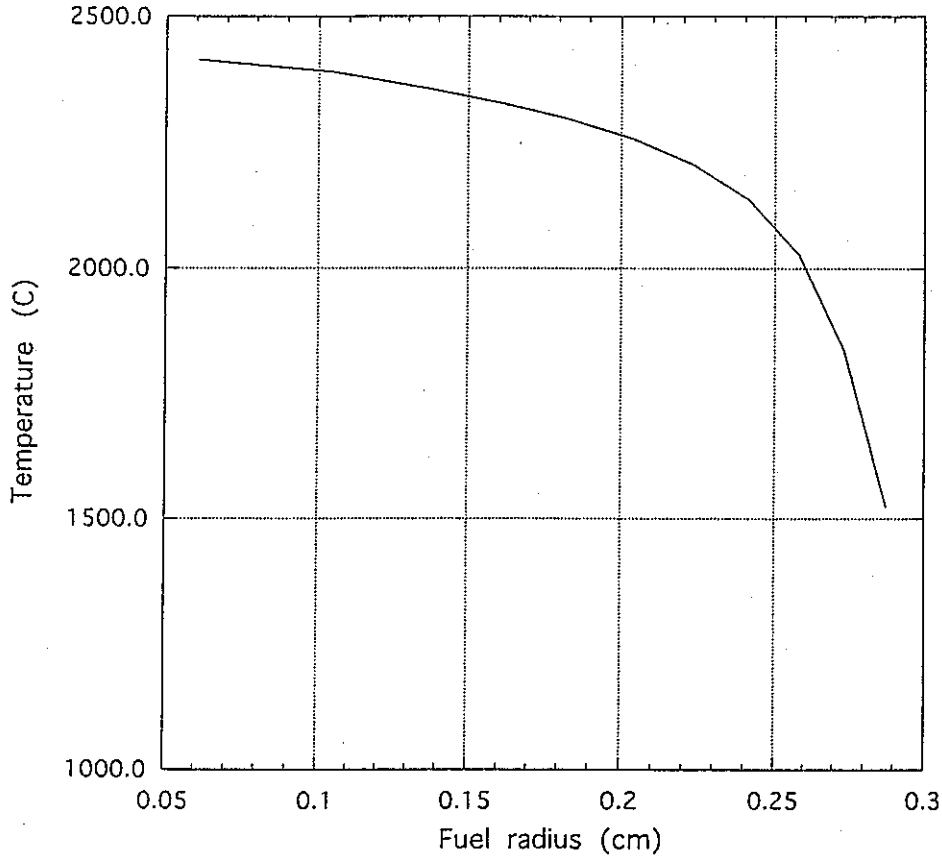

Fig.4 Calculated fuel temperature at PPN at 385 ms after TOP triggering

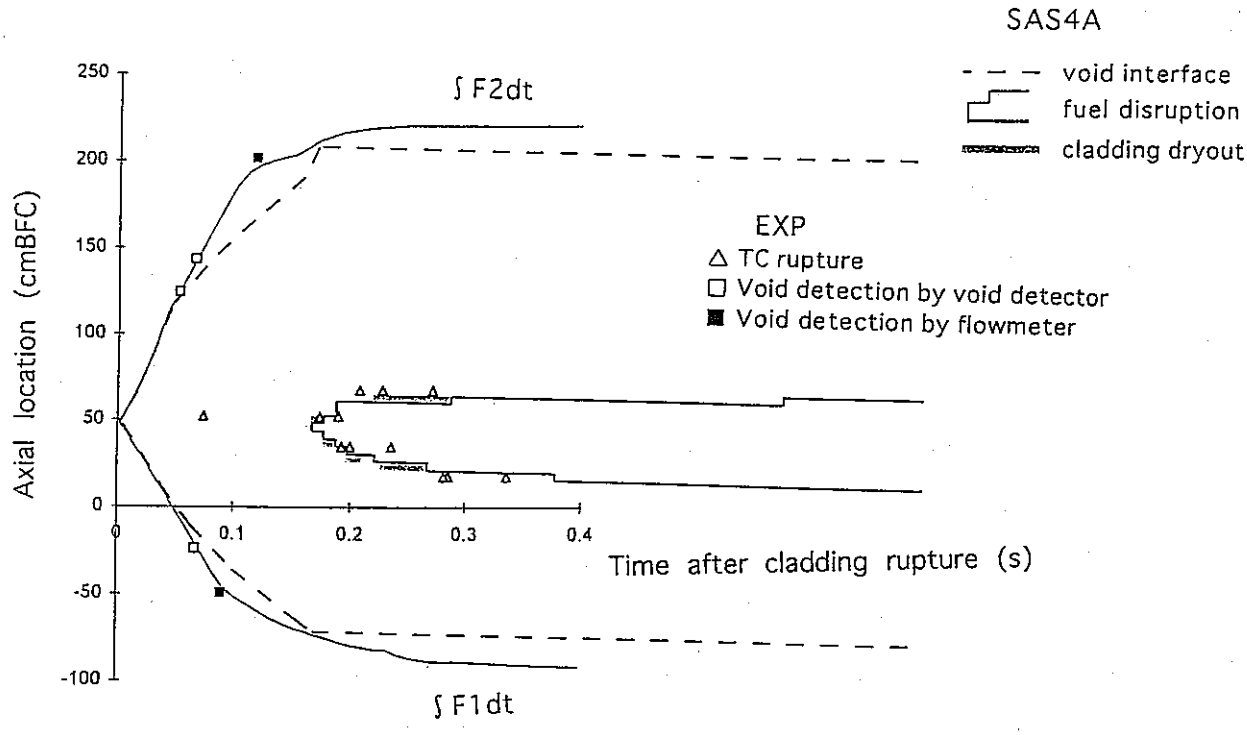

Fig.5 Coolant-channel voiding, cladding dryout and fuel disruption calculated with SAS4A

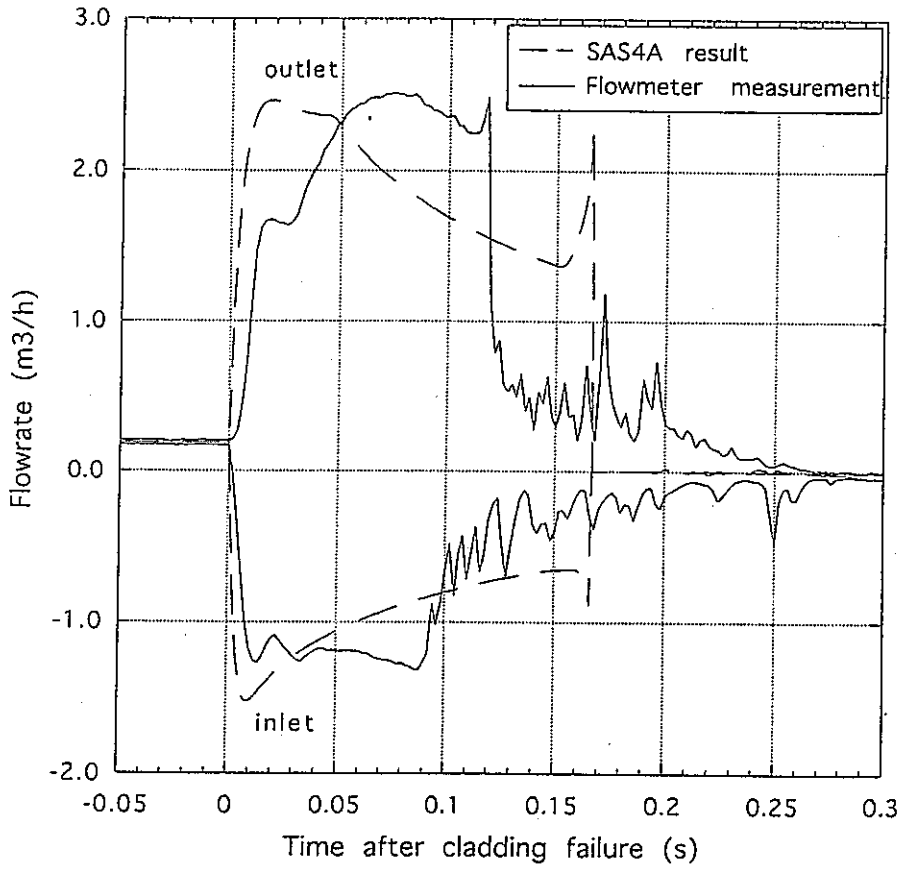

Fig.6 Coolant flowrate response after the cladding failure

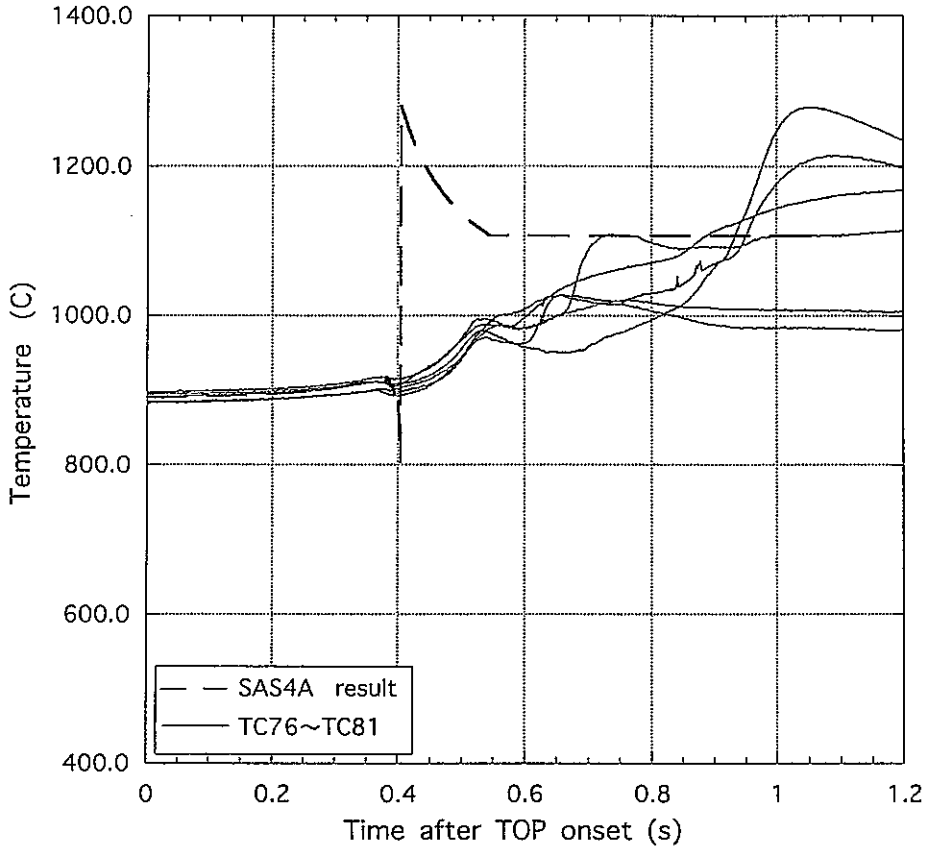

Fig.7 History of coolant-channel temperature at TFC

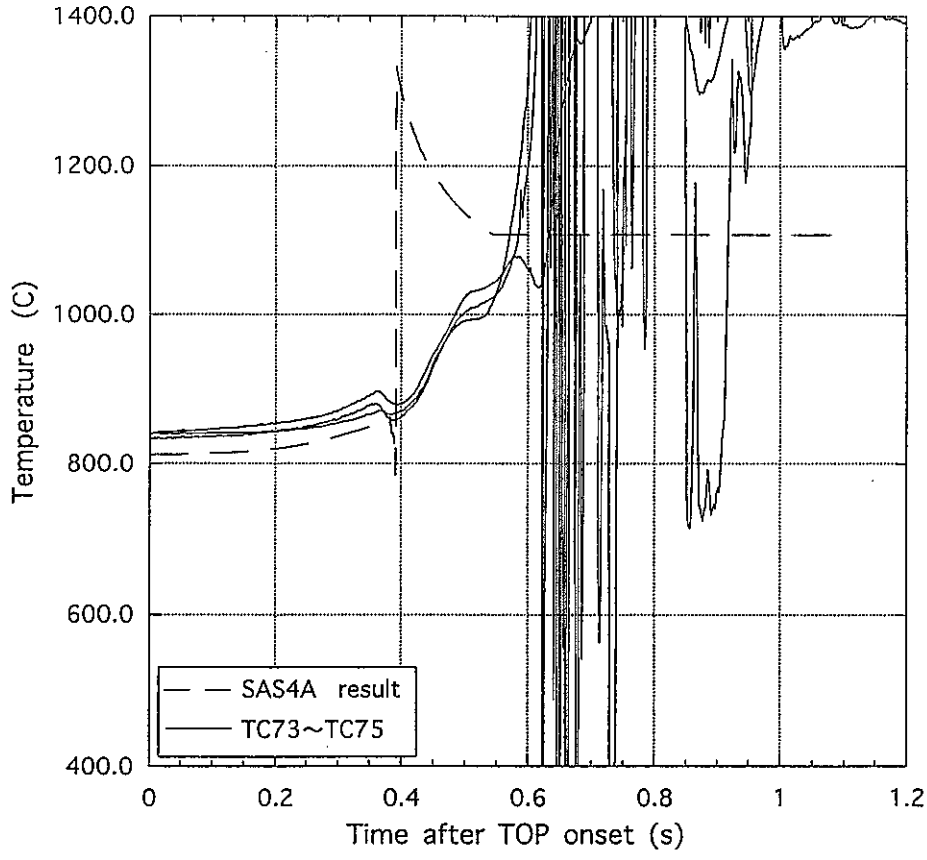

Fig.8 History of coolant-channel temperature at 67cmBFC

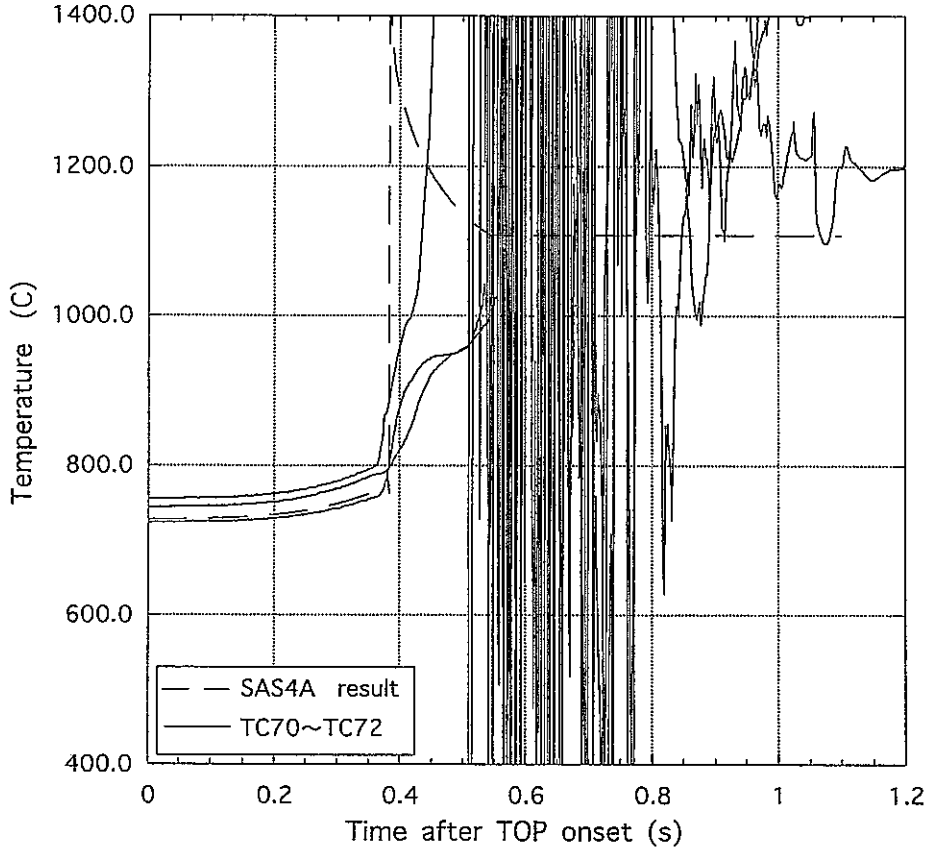

Fig.9 History of coolant-channel temperature at 52cmBFC

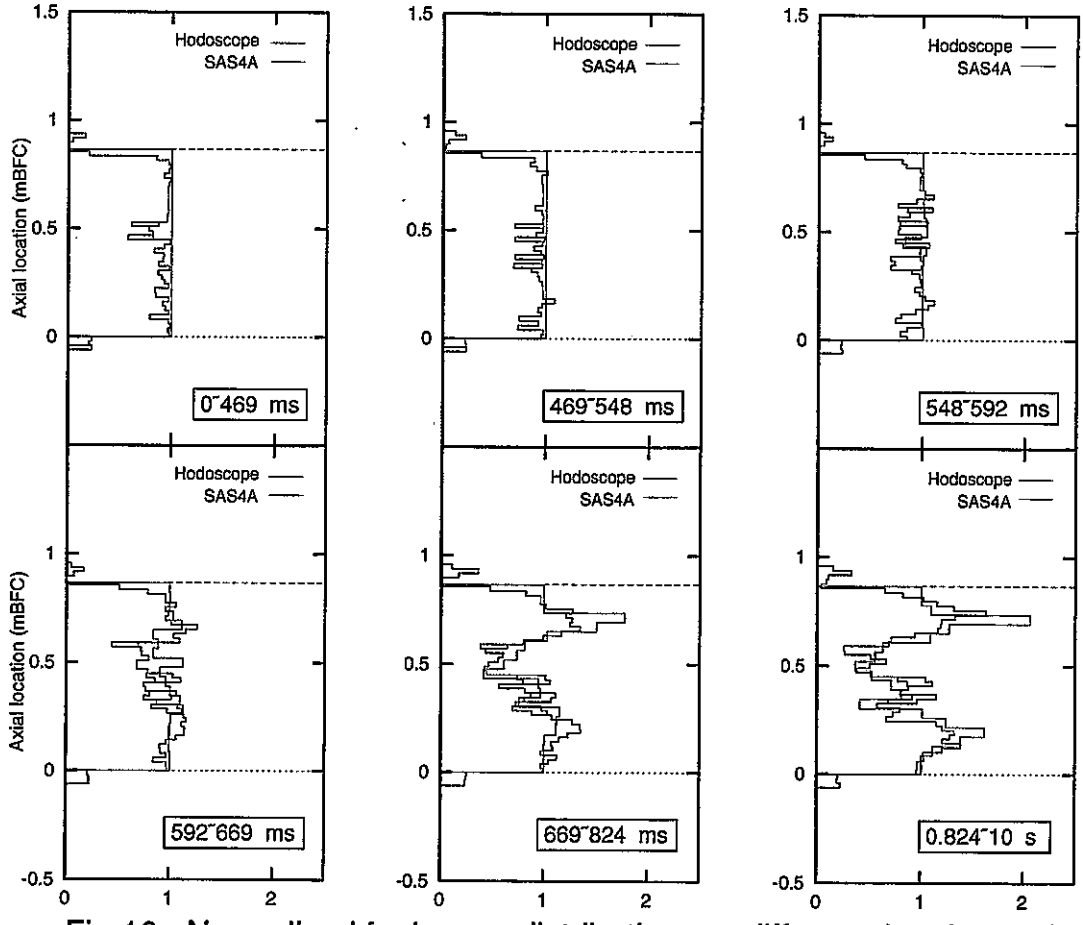

Fig.10 Normalized fuel mass distributions at different time intervals

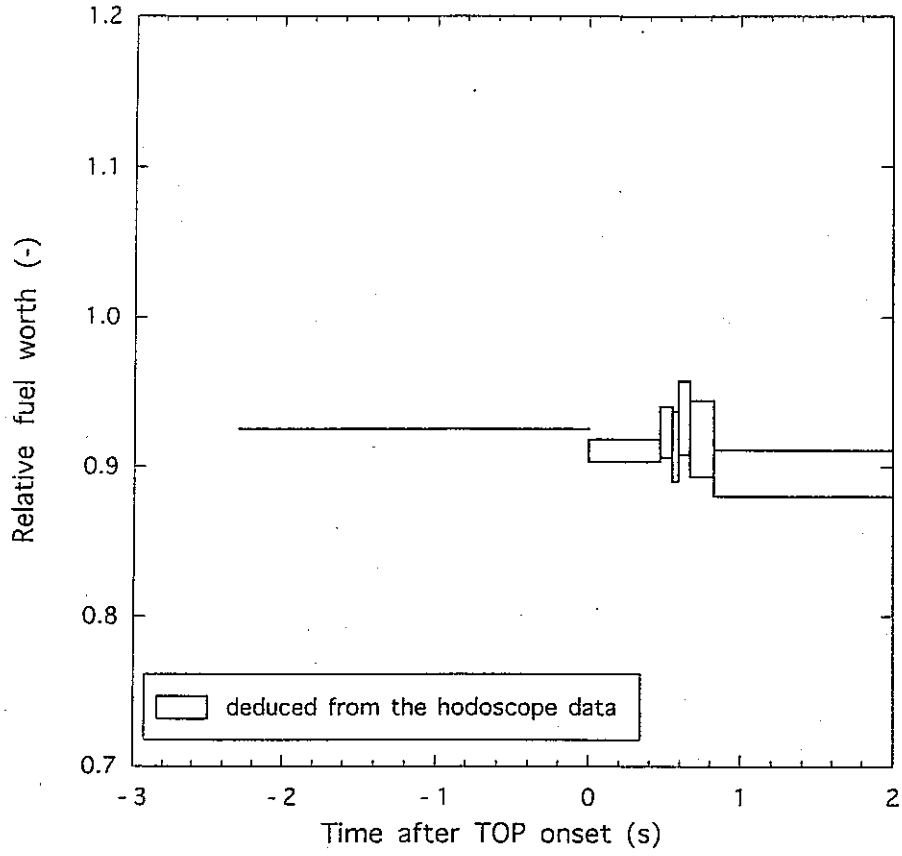

Fig.11 Relative fuel worth during LOF and TOP deduced from the hodoscope data

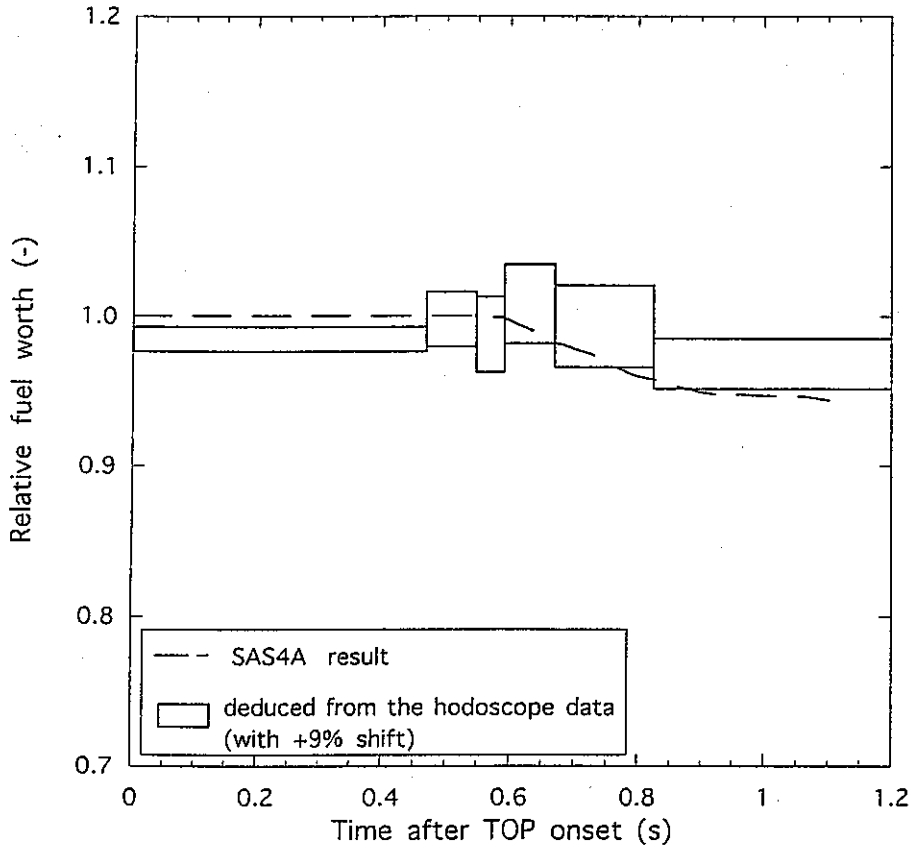

Fig.12 Comparison of relative fuel worth during TOP between analysis and hodoscope data

Appendix Temporary modifications adopted in this study

In the present study, simulation of gas release from the failed fuel pin before fuel melting is intended. The plenum-gas-blowout model is used here as a basic tool for this simulation. However, plenum gas blowout always takes place after coolant-channel voiding which is quite different from the LT1 condition at failure. Because of this irregular utilization of the gas-blowout model, some specific modifications were necessary.

A-1 Prevention of vapor condensation

In the SAS4A model, condensation of gas mixture (fission gas and sodium vapor) is calculated with different methods for different phases. After molten fuel ejection or fuel disruption, the PLUTO or LEVITATE module is used. In these post-failure modules, fission gas and sodium vapor are separately defined. However, before entering into these modules, coolant-boiling model is used, where gas released into the coolant channel is represented with additional sodium vapor.

a) Before entering into PLUTO or LEVITATE

Although the gas term is not included in the basic model framework, a virtual gas fraction is defined based on the gas-release history. This virtual gas fraction can be used for simulation of non-condensable characteristic of gas with a reduced condensation heat-transfer coefficient. However, this treatment is not applicable to the completely non-condensable gas. With the present model, even with a 100% of virtual gas fraction, some sodium condensation is allowed and it prevented realistic simulation of the LT1 test. In order to simulate the completely non-condensable characteristic of LT1 gas bubble, a very low condensation heat-transfer coefficient is adopted in this study. This is performed introducing HCHELP=1.0E-12 in the subroutine TSC3.

With this treatment, sodium condensation can be prevented. However, suppression of condensation accompanies suppression of heat transfer between the bubble and structures including the pin.

b) In the LEVITATE module

In the PLUTO or LEVITATE module, although fission gas is modeled in fact, presence of fission-gas within the coolant channel before PLUTO or LEVITATE initiation is not defined. Therefore, at the initiation of the

LEVITATE module in the LT1 case, gas mass in the coolant channel becomes zero. With this definition, the reference model results in sudden increase of sodium condensation.

In order to suppress the condensation in the LEVITATE module, sodium condensation-heat-transfer coefficient CFNACN is set to zero. With CFNACN=0.0, a divide check occurs in the subroutine LETRAN in a part where the thermal resistance is defined as an inverse of conductance. Therefore, in order to avoid this trouble, a very small value is given for the conductance term (if CONNEW.eq.0.0 CONNEW=1E-20).

Sodium evaporation is also suppressed in this study adopting a very low value for the sodium evaporation-heat-transfer coefficient CFNAEV, to avoid unexpected dryout, which is not necessary because the cladding is already behaving as adiabatic to the coolant channel.

A-2 Correction for coolant-slug-number definition

The plenum gas blowout takes place usually after certain duration of coolant boiling so that presence of saturated sodium is implicitly assumed. However, in the LT1 test analysis, sodium vapor representing the released gas has temperature lower than saturation. Under this irregular situation, initial definition of liquid-coolant-slug number KLQN in the subroutine TSCBUB is not appropriate. Therefore, in the present study, initial KLQN definition is corrected as a temporary treatment.

A-3 Specification of plenum gas mass for blowout

With the QUASAR sibling pin, total gas amount within the upper and lower plena is estimated to have been 1.35 g, which is roughly corresponding to the gas used for channel voiding in the LT1 test. This means the main part of gas present in the lower plenum was released into the coolant channel within the relatively short time range. However, this realistic blowout-gas amount results in liquid slug disappears from the presently modeled field which is not representing the whole test section appropriately. This liquid-slug disappearance within the presently modeled field gives difficulty to continue the calculation. In order to avoid this difficulty, 0.8 g is adopted in this study as the plenum-gas source term for blowout. This is defined as PLGMS=0.8E-3 within the subroutine TSBOIL.